

SYNCHRONOUS GENERATOR NO-LOAD VOLTAGE PREDICTION USING A COMBINED ANALYTICAL AND FEM APPROACH

S. Keller, M. Tu Xuan, J.-J Simond

Ecole Polytechnique Fédérale de Lausanne (EPFL)
Laboratoire de Machines Electriques
CH-1015 Switzerland
Email: stefan.keller@epfl.ch

Abstract - A combined analytical and FEM method for prediction of the no-load voltage waveform of laminated salient pole synchronous generators is presented in this article.

Very precise prediction of the no-load voltage, including saturation effects as well as the effects of the currents in the damper bars is achieved by combination of magnetostatic 2D finite element simulations for calculating the magnetic coupling between the machine windings and of an analytical resolution. At the same time simulation time is drastically reduced, compared to transient magnetic 2D finite element simulations.

The method was verified on several examples, comparing the obtained results (damper bar currents and no-load voltage) to results obtained from transient magnetic finite element simulations and in one case to the measured no-load voltage.

1. INTRODUCTION

A fast and reliable prediction of the no-load voltage waveform of salient pole synchronous generators is very important for the designer. Knowing in advance the harmonics content of the no-load voltage is essential for satisfying standards requirements (Telephone Harmonic Factor, etc.). Another important point during the design is the prediction of the losses due to currents in the damper bars, induced by the slot pulsation field.

There exist presently different analytical, numerical and combined methods addressing these problems. Traxler-Samek, Schwery and Schmidt [1] apply a fast analytical method, whose output can be used as a criteria for the selection of the number of stator slots. On the other extreme, transient finite element simulations allow very precise prediction, not only of the no-load voltage waveform, but also of the damper bar currents or of the magnetization of the machine. In [2] transient finite element analysis is used for prediction of the no-load voltage shape and in [3] this same method is used for the design of the damper winding of a single-phase generator. As this method is very time-consuming, especially in the case of a fractional slot stator winding, it is not very suitable for comparing several different machine geometries. Also a certain number of combined methods were presented. In [4] a combined analytical and finite element modeling method is used for calculation of the currents induced in the damper winding and for calculation of the force-density harmonics including the effects of these currents. Finally in [5] and [6] the modified winding function approach and the magnetics

circuits approach have been used for modeling the synchronous machine performance under dynamic air-gap eccentricity.

The authors will present in this article a combined analytical and finite element method for prediction of the damper bar currents and the voltage waveform in no-load conditions. The described method takes into account saturation effects as well as all geometrical data of the machine (except effects of the end regions). For verification of the method, the results obtained were compared to the results obtained from transient finite element simulations and, in one case, to the measured no-load voltage. These comparisons were done on several synchronous generators, in the range from 10MVA to 30MVA, including integer and fractional slot stator windings, and damper windings centered or shifted on the pole shoes. The described method was implemented in a tool, which is currently used by one of our major industrial partners. A generalization of the method for analyzing various rotor eccentricity and stator deformation conditions in synchronous machines is in development.

Summarized, the method consists in calculating, using magnetostatic 2D finite element simulations, the magnetic coupling of the machine electrical conductors (damper bars, field and stator windings) for a certain number of positions of the rotor, considering the machine rotational periodicity. In a second step the damper bar currents and the no-load voltage can be calculated by solving the differential equation system formed of the inductances calculated in the first step.

2. MAGNETIC COUPLING OF THE MACHINE CONDUCTORS

Due to magnetic coupling a voltage is induced in each conductor of the machine. The voltage induced in conductor 'j' is given by the derivative of the flux seen by conductor 'j':

$$v_j = \frac{d\phi_j}{dt} \quad (1)$$

The flux seen by the conductor 'j' (damper bar or conductor on the stator) can be expressed as the sum of the flux contributions of the currents in the field windings and in the 'N' damper bars. As the MMF caused by the damper bar currents is significantly lower than the MMF caused by the current in the field windings, the flux created by the damper bar currents is supposed not to influence the level of saturation of the generator. Therefore the contribution of the damper bar 'k' can be expressed as the multiplication of the current in the damper bar 'k' with a mutual differential inductance, describing the change in flux seen by conductor 'j' when the current in the damper bar 'k' changes:

$$\phi_j = \phi_{exc,j} + \sum_{k=1}^N \phi_{k,j} = \phi_{exc,j} + \sum_{k=1}^N L_{diff_{k,j}} i_k \quad (2)$$

These differential inductances depend on the rotor position and on the saturation of the machine. Thus, they have to be determined for a given main flux (given field current) and for different rotor positions. As the stator has, as seen from the rotor, a rotational periodicity of one stator slot pitch, the inductances have to be determined only for some positions of the rotor within one stator slot pitch.

The inductances are obtained using magnetostatic 2D finite element simulations. For the determination of $L_{diff_{k,j}}$ the results of two finite element simulations are necessary: one with the field windings supplied with the current corresponding to the chosen main flux and one with the field windings supplied with the same current and with damper bar 'k' supplied with a test current. $L_{diff_{k,j}}$ is then calculated as follows:

$$L_{diff_{k,j}} = \frac{\phi_{exc,k,j} - \phi_{exc,j}}{i_k} \quad (3)$$

Where:

$\phi_{exc,k,j}$: flux created by the field windings and the current in conductor 'k', seen by conductor 'j'

$\phi_{exc,j}$: flux created only by the field windings, seen by conductor 'j'

As each simulation can be used for the calculation of several inductances, the necessary number of magnetostatic finite element simulations is: $(N+1)W$, where 'N' is the number of damper bars and 'W' is the number of rotor positions considered within one stator slot pitch. The simulations with only the field windings supplied provide also the values of flux caused by the current in the field windings (as used in equation 2). As in the case of transient finite element simulations, only a part of the machine has to be considered, therefore a typical number of magnetostatic finite element simulations could be: $(20+1)20 = 420$ (one pole pair, 10 damper bars per pole, 20 positions of the rotor).

Using magnetostatic finite element simulations to determine the magnetic coupling of the machine electrical conductors allows to take into account precisely saturation effects as well as all geometrical data of the machine (pole shoe shape, rotor and stator slotting, damper bar distribution, etc.) except end region effects. All these influencing factors are contained in the values of flux and in the differential inductances which can be calculated using a standardized scheme of magnetostatic finite element calculations for any type of salient-pole synchronous generator (integer and fractional slot stator windings, various damper bar distributions, various pole shoe shapes, etc.).

3. ELECTRICAL CIRCUIT OF THE DAMPER CAGE AND CALCULATION OF THE DAMPER BAR CURRENTS

The machine conductors form the following 3 galvanically separated circuits:

- Field windings
- Damper cage
- Stator windings

As the current in the field windings is considered constant and the machine is considered in no-load conditions, the field windings and the stator windings do not have to be modeled. The electrical circuit of figure 1 is associated with the damper cage.

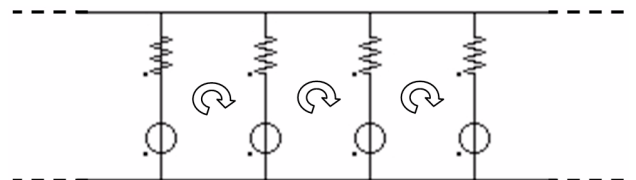


Figure 1. Electrical circuit associated with the damper cage

In figure 1 only a part of the damper circuit is shown, the whole circuit consists of one branch for each damper bar present in the part of the machine considered for calculation of the inductances, as described in paragraph 2. As can be seen in figure 1, each damper bar is modeled as one branch composed of a resistance and a voltage source. The resistance models obviously the resistance of the damper bar and the voltage source models the voltage induced, which is the derivative of the flux seen by the damper bar (as in equation 1). The resistance of the short circuit rings is neglected but could also be considered, changing slightly the equations described below.

For each loop in the electrical circuit the following equation can be written:

$$R_{\text{bar}_j} i_{\text{bar}_j} - R_{\text{bar}_{j+1}} i_{\text{bar}_{j+1}} + \frac{d\varphi_j}{dt} - \frac{d\varphi_{j+1}}{dt} = 0 \quad (4)$$

The flux seen by each one of the two bars, φ_j and φ_{j+1} , can be replaced with the expression of equation 2 and the derivative in time of the flux terms in equation 2 can be replaced with its partial derivatives as follows:

$$\frac{d\varphi_{i,j}}{dt} = \frac{\partial \varphi_{i,j}}{\partial i_i} \frac{di_i}{dt} + \frac{\partial \varphi_{i,j}}{\partial \alpha} \Omega \quad (5)$$

Where α is the position of the rotor and its derivative in time the rotating speed Ω . The derivation of the flux with respect to the current can be replaced with a differential inductance as described in paragraph 2:

$$\frac{\partial \varphi_{i,j}}{\partial i_i} = L_{\text{diff}_{i,j}} \quad (6)$$

Therefore and expressing $\varphi_{i,j}$ also using the differential inductances:

$$\frac{d\varphi_{i,j}}{dt} = L_{\text{diff}_{i,j}} \frac{di_i}{dt} + \frac{\partial L_{\text{diff}_{i,j}}}{\partial \alpha} i_i \Omega \quad (7)$$

The following equation is obtained for each loop of figure 1:

$$R_{\text{bar}_j} i_{\text{bar}_j} - R_{\text{bar}_{j+1}} i_{\text{bar}_{j+1}} + \frac{d\varphi_{\text{exc},j}}{dt} + \sum_{k=1}^N \left(L_{\text{diff}_{k,j}} \frac{di_k}{dt} + \frac{\partial L_{\text{diff}_{k,j}}}{\partial \alpha} i_k \Omega \right) - \left(\frac{d\varphi_{\text{exc},j+1}}{dt} + \sum_{k=1}^N \left(L_{\text{diff}_{k,j+1}} \frac{di_k}{dt} + \frac{\partial L_{\text{diff}_{k,j+1}}}{\partial \alpha} i_k \Omega \right) \right) = 0 \quad (8)$$

Finally the current in the last bar can be expressed as the negative sum of the currents in all other damper bars (Kirchhoffs law):

$$R_{\text{bar}_j} i_{\text{bar}_j} - R_{\text{bar}_{j+1}} i_{\text{bar}_{j+1}} + \sum_{k=1}^{N-1} \frac{di_k}{dt} (L_{\text{diff}_{k,j}} - L_{\text{diff}_{N,j}} - L_{\text{diff}_{k,j+1}} + L_{\text{diff}_{N,j+1}}) + \Omega \sum_{k=1}^{N-1} i_k \left(\frac{\partial L_{\text{diff}_{k,j}}}{\partial \alpha} - \frac{\partial L_{\text{diff}_{N,j}}}{\partial \alpha} - \frac{\partial L_{\text{diff}_{k,j+1}}}{\partial \alpha} + \frac{\partial L_{\text{diff}_{N,j+1}}}{\partial \alpha} \right) + \frac{d\varphi_{\text{exc},j}}{dt} - \frac{d\varphi_{\text{exc},j+1}}{dt} = 0 \quad (9)$$

As all the $L_{\text{diff}_{k,j}}$ and $\varphi_{\text{exc},j}$ have been determined as described in paragraph 2 and the only remaining unknowns being the damper bar currents, the system of differential equations formed of $N-1$ equations (where 'N' is the number of damper bars, the current in the last bar being calculated as mentioned above) of the type of equation 9 can be solved using a numerical method (in the case of this article the 2nd order Runge-Kutta method was used).

The described method could also be used in the case of several galvanically separated damper cages (e.g. one on each pole shoe) or in the case of parallel circuits on the stator including the effects of currents circulating in the parallel circuits in no-load conditions (especially in the case of an eccentric rotor). In these cases the equations described above have to be modified.

4. CALCULATION OF THE NO-LOAD VOLTAGE

Having calculated the currents in all damper bars, the no-load voltage in each phase can be obtained by summing the derivatives of the flux seen by each conductor of the phase. The flux seen by each conductor can again be expressed as the sum of the contributions of the field windings and the 'N' damper bars (as in equation 2). In the case of the conductors on the stator the differential inductances and the values of flux caused by the field windings, calculated for some rotor positions within one stator slot pitch, have to be re-assigned to the conductors on the stator after a rotation of the rotor of one stator slot pitch, for taking into account the new initial position of each conductor. This technique allows to use the magnetic coupling, calculated only for some rotor positions within one stator slot pitch, for any position of the rotor as well as for any kind of winding distribution.

The following formula was used for the numerical derivation of the flux:

$$\frac{d}{dt} \varphi_j(t_k) \cong \frac{\varphi_j(t_k) - \varphi_j(t_{k-1})}{t_k - t_{k-1}} \quad (10)$$

5. COMPARISON OF THE RESULTS

The damper bar currents and the no-load voltage obtained using the described method were compared to the currents and the voltage obtained from 2D transient finite element simulations and in one case also to the measured no-load voltage.

Figures 2 and 3 compare the no-load voltage waveform of an existing generator (6.3kV, 11MVA, 750rpm, 50Hz, integer slot stator winding) obtained using the described method to the no-load voltage obtained from transient finite element simulations. Figure 4 compares the no-load voltage harmonics (in % of the fundamental) of the same generator, this time also to the harmonics of the measured no-load voltage.

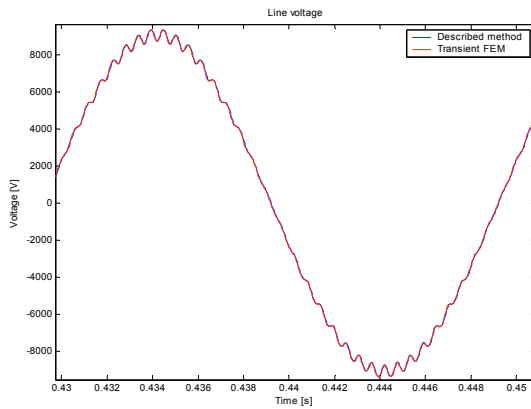


Figure 2. Comparison of the no-load voltage waveform

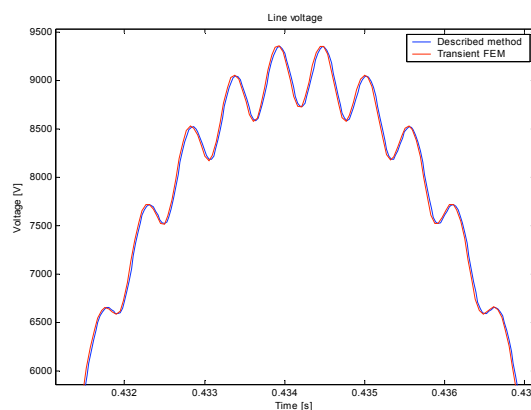


Figure 3. Comparison of the no-load voltage, detail

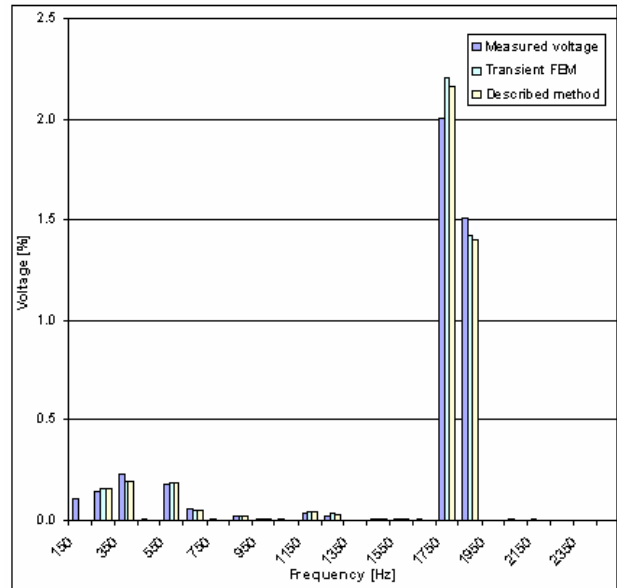


Figure 4. Comparison of the no-load voltage harmonics

A very good agreement of the results can be observed, not only comparing the described method to transient finite element analysis, but also comparing to the measured values.

Figure 5 shows a comparison of the currents in two adjacent damper bars, obtained using the described method to the current obtained from transient finite element simulations. Also in this case the agreement is very good, therefore the no-load losses due to currents in the damper bars can be predicted very precisely.

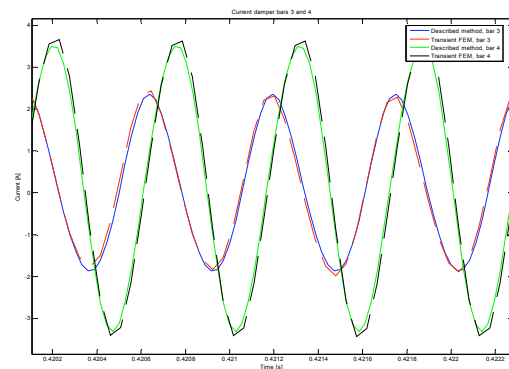


Figure 5. Comparison of the currents in two adjacent damper bars

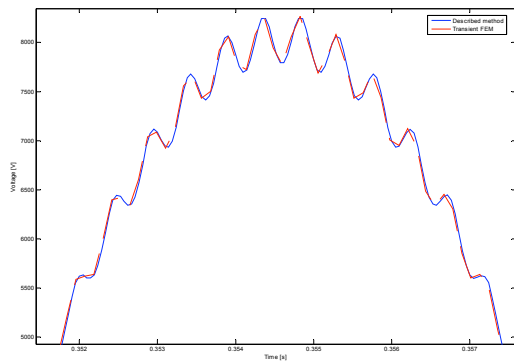


Figure 6. Comparison of the no-load voltage waveform

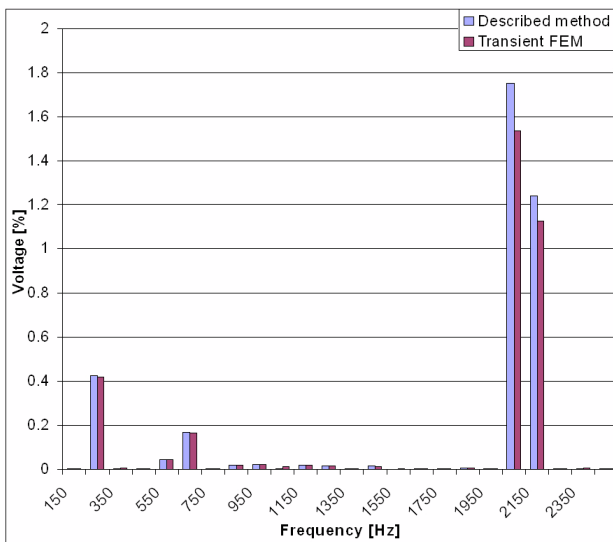


Figure 7. Comparison of the no-load voltage harmonics

Figures 6 and 7 show a comparison of the no-load voltage waveform and harmonics of another existing generator (5.5kV, 15MVA, 500rpm, 50Hz, fractional slot stator winding). The slightly higher difference in the case of the harmonics due to the slot pulsation field are probably due to the low sampling rate chosen for the transient finite element calculation.

All calculations were performed on a desktop PC with Pentium 4 CPU (2.6GHz, HT) and 1GB of RAM, running Windows XP Professional. The calculations applying the described method (including the magnetostatic finite element calculations) were about 20 times faster than the transient finite element simulations performed for comparison.

In the case of the described method, the magnetostatic finite element calculations occupy the major part of the calculation time. Therefore the calculation time depends heavily on the number of damper bars present in the circuit as well as on the number of rotor positions considered within one stator slot period (as described in paragraph 2.).

6. CONCLUSION

The modeling method presented in this article allows the prediction of the damper bar currents and of the no-load voltage of laminated salient-pole synchronous generators with almost the same precision as transient finite element simulations. At the same time simulation time was reduced by a factor of about 20. The magnetostatic finite element simulations, necessary for the determination of the magnetic coupling of the machines conductors, can be automatized and the calculation of the damper bar currents and the no-load voltage, based on the results of the finite element simulations has been implemented in a user-friendly, graphical tool, allowing comfortable application of the method. This tool is currently used by one of our major industrial partners.

In a next stage the method will be modified for analysis of the effects of various types of rotor eccentricity conditions and stator deformations in salient-pole synchronous generators.

REFERENCES

- [1] G. Traxler-Samek, A. Schwery, E. Schmidt, "Analytic Calculation of the Voltage Shape of Salient Pole Synchronous Generators Including Damper Winding and Saturation Effects", Proceedings of the 15th International Conference on Electrical Machines (ICEM), 2002
- [2] A. Schwery, G. Traxler-Samek, E. Schmidt, "Application of a Transient Finite Element Analysis with Coupled Circuits to Calculate the Voltage Shape of a Synchronous Generator", Proceedings of the 10th IEEE Conference on Electromagnetic Field Computation (CEFC), 2002
- [3] K. Weeber, "Design of Amortisseur Windings of Single-Phase Synchronous Generators Using Time-Stepping Finite Element Simulations", International Conference on Electrical Machines (ICEM), 1998
- [4] A. M. Knight, H. Karmaker, K. Weeber, "Use of a Permeance Model to Predict Force Harmonic Components and Damper Winding Effects in Salient-Pole Synchronous Machines", IEEE Transactions on Energy Conversion, Vol. 17, No. 4, 2002
- [5] H. A. Toliyat, N. A. Al-Nuaim, "Simulation and Detection of Dynamic Air-Gap Eccentricity in Salient-Pole Synchronous Machines", IEEE Transactions on Industry Applications, Vol. 35, No. 1, 1999
- [6] I. Tabatabaei, J. Faiz, H. Lesani, M. T. Nabavi-Razavi, "Modeling and Simulation of a Salient-Pole Synchronous Generator With Dynamic Eccentricity Using Modified Winding Function Theory, IEEE Transactions on Magnetics, Vol. 40, No. 3, 2004